Atmos. Chem. Phys. Discuss., 10, 1193–1220, 2010
www.atmos-chem-phys-discuss.net/10/1193/2010/

Atmospheric Chemistry and Physics Discussions

This discussion paper is/has been under review for the journal Atmospheric Chemistry and Physics (ACP). Please refer to the corresponding final paper in ACP if available.

Sunphotometry of the 2006–2007 aerosol optical/radiative properties at the Himalayan Nepal Climate Observatory – Pyramid (5079 m a.s.l.)

G. P. Gobbi[1], F. Angelini[1], P. Bonasoni[2], G. P. Verza[3], A. Marinoni[2], and F. Barnaba[1]

[1]Institute of Atmospheric Sciences and Climate CNR, Rome, Italy
[2]Institute of Atmospheric Sciences and Climate CNR, Bologna, Italy
[3]Ev-K2-CNR Organization, Bergamo, Italy

Received: 3 December 2009 – Accepted: 22 December 2009 – Published: 18 January 2010

Correspondence to: G. P. Gobbi (g.gobbi@isac.cnr.it)

Published by Copernicus Publications on behalf of the European Geosciences Union.

Abstract

In spite of being located at the heart of the highest mountain range in the world, the Himalayan Nepal Climate Observatory (5079 m a.s.l.) at the Ev-K2-CNR Pyramid is shown to be affected by the advection of pollution aerosols from the populated regions of southern Nepal and the Indo-Gangetic plains. Such an impact is observed along most of the period April 2006–March 2007 addressed here, with a minimum in the monsoon season. Backtrajectory-analysis indicates long-range transport episodes occurring in this period to originate mainly in the West Asian deserts. At this high altitude site, the measured aerosol optical depth is observed to be: 1) about one order of magnitude lower than the one measured at Gandhi College (60 m a.s.l.), in the Indo-Gangetic basin, and 2) maximum during the monsoon period, due to the presence of elevated (cirrus-like) particle layers. Assessment of the aerosol radiative forcing results to be hampered by the persistent presence of these high altitude particle layers, which impede a continuous measurement of both the aerosol optical depth and its radiative properties from sky radiance inversions. Even though the retrieved absorption coefficients of pollution aerosols was rather large (single scattering albedo of the order of 0.6–0.9 were observed in the month of April 2006), the corresponding low optical depths (~0.03 at 500 nm) are expected to limit the relevant radiative forcings. Still, the high specific forcing of this aerosol and its capability of altering snow surface albedo provide good reason for continuous monitoring.

1 Introduction

The net radiative effect of anthropogenic aerosols currently present in the atmosphere is to cool the Earth system by increasing its albedo (e.g., Forster et al., 2007; Bellouin et al., 2008). However, some of these aerosols absorb radiation and warm the atmospheric layers they are suspended within. In highly polluted regions, dominance of the absorption effect can lead to a positive climate forcing, that is, a warming effect

ACPD

10, 1193–1220, 2010

(Satheesh and Ramanathan, 2000; Ramanathan et al., 2007; Nakajima et al., 2007; Ramanathan and Carmichael, 2008). Light absorption by aerosols is mainly due to the black carbon (BC) and organic particulate produced by the combustion of fossil fuels or biomasses. Air masses containing such aerosols are also referred to as atmospheric brown clouds (ABC, e.g., Ramanathan and Crutzen, 2003). Major sources of absorbing, BC aerosols are South and North America, Europe, Central and South Africa, South and East Asia (e.g., Ramanathan and Carmichael, 2008).

In the Indian sub-continent, a positive aerosol forcing has been reported by several authors, e.g., at Kanpur in the Indo-Gangetic (IG) basin (Chinnam et al., 2006; Dey and Tripathi, 2008), in the wintertime at Manora Peak in the Central Himalayas (Pant et al., 2006), and in Nepal (Ramana et al., 2004). A positive forcing was also observed in the aerosol-laden air proceeding from the Indian continent to the Maldives during the pre-monsoon (biomass burning) season, and proposed as a possible cause for the observed retreat of the Himalayan glaciers (Ramanathan et al., 2007). In addition to pollution, the aerosol load of northern India and Nepal is affected by important natural contributions: mineral dust from the surrounding West Asian deserts (or even from the Sahara and Arabian ones) can constitute a large fraction of the aerosol optical depth (AOD), particularly during the pre-monsoon season (March–May), when dust is observed to mix with anthropogenic pollution (e.g., Shresta et al., 2000; Chinnam et al., 2006; Prasad and Singh, 2007; Liu et al., 2008; Verma et al., 2008). In this context, the assessment of the radiative effects of anthropogenic vs. natural aerosols in this region represents an intricate task (e.g., Dey and Tripathi, 2008). Clouds add uncertainty to such assessment, since they constitute an important modulator of radiation, particularly important during the monsoon season (e.g., Liu et al., 2008).

Determination of the direct radiative forcing of aerosols essentially requires the knowledge of their scattering and absorption optical depths, plus ground albedo (e.g., Haywood and Boucher, 2000; Nakajima et al., 2007). In this respect, the magnitude of the radiative forcing is proportional to the AOD, and this latter is about an order of magnitude smaller at the high mountain sites with respect to the IG plains (e.g.,

ACPD
10, 1193–1220, 2010

Ramana et al., 2004; Pant et al., 2006). Sun-pointing photometers provide spectral measurements of the AOD, which is the sum of the scattering (AOD_{sca}) and absorption (AOD_{abs}) components (e.g., Holben et al., 1998). Sky-scanning sunphotometers permit the separation of these two components and the measurement of the single scattering albedo (SSA=$AOD_{sca}/(AOD_{sca}+AOD_{abs})$, e.g., Dubovik and King, 2000). Over typical vegetated soil albedos, the switching from a negative (cooling) to a positive (warming) aerosol radiative forcing takes place for SSA descending below ∼0.9 (i.e., for highly absorbing aerosols). This threshold rises to SSA ∼0.95 (i.e., most of anthropogenic and mineral aerosols) over the highly-reflecting surfaces of snow and/or deserts (e.g., Haywood and Boucher, 2000).

The absorbing properties of aerosols reaching the Himalayan region have been studied by few authors: wintertime large abundances of black carbon, BC ($1.36\pm0.99\,\mu g\,m^{-3}$ in December) observed by Pant et al. (2006) at Manora Peak (1950 m a.s.l.) in the Central Himalayas was found to originate from the human activities in the adjoining valleys and to boundary layer transport. Since Manora Peak is located at 10 km from nearby valley villages laying at some 300 m a.s.l., such an impact is somewhat expected. In Nepal, high aerosol absorption (SSA in the range 0.7–0.9) was reported by Ramana et al. (2004), during a winter 2002 campaign carried-out in Kathmandu and nearby locations. More remote conditions have been described by Shresta et al. (2000) who observed wintertime, pre and early-monsoon accumulation of pollutants to occur also at the high elevation site of Phortse (4100 m a.s.l.), in the Eastern Nepalese Himalayas Gokyo Valley. They attributed such condition to the regional circulation-transported pollutants from the Indian-Nepalese plains to this high Himalayan site.

The Nepal Climate Observatory at the Pyramid (NCO-P, http://evk2.isac.cnr.it), established in March 2006 at 27.9° N, 86.8° E, 5079 m a.s.l. in the high Khumbu valley (Bonasoni et al., 2010), provided us with an opportunity to study such pollution-transport conditions by means of both sunphotometer and in situ observations of aerosol radiative and chemical properties at an even more remote location at the heart

of the Himalayas (e.g., Fig. 1). The NCO-P was set up by the Ev-K2-CNR organization in the framework of the SHARE (Stations of High Altitude for Research on the Environment, http://www.evk2cnr.org/cms/en) and ABC-UNEP (http://www.rrcap.unep.org/abc/) programs. ISAC-CNR selected and installed the instrumentation for the atmospheric observations at the NCO-P, located at the top of a hill overlooking the Ev-K2-CNR Pyramid (Bonasoni et al., 2008). In this paper we analyse the first year of sunphotometer observations carried-out at the Observatory to identify the seasonal patterns of the aerosol column above this area and infer the main drivers of its radiative properties. To this aim, we shall also employ: 1) black carbon and aerosol size distribution measurements carried out at the NCO-P (e.g., Marinoni et al., 2010), 2) sunphotometer observations carried out at Gandhi College (GC), in the Indo-Gangetic plains, e.g., Fig. 1; 3) NOAA-Hysplit backtrajectories, 4) fires observations from the MODIS sensor onboard the NASA-Terra satellite, and 5) satellite aerosol observations retrieved by the orbiting CALIOP lidar.

2 Methods

2.1 The sunphotometer

Our automated Cimel CE-318 sunphotometer was installed at the NCO-P on 27 March 2006, as part of the AERONET network (Holben et al., 1998). The sunphotometer operates at seven wavelengths (340, 380, 440, 500, 670, 870, 940 and 1020 nm), performing both "direct sun" and "sky radiance" measurements. Data are continually sent via GMS Satellite to the AERONET headquarters at NASA-GSFC for processing. Standard products of the sun-pointing data analysis are aerosol optical depths (AOD) and related Angstrom exponents at all the wavelengths, plus precipitable water (PW) (Holben et al., 1998), and aerosol fine mode optical depth (AOD_{FM}) at 500 nm (O'Neill et al., 2003). In addition, inversion of *almucantar* measurements of sky radiance retrieves aerosol size distribution, asymmetry factor and single scattering albedo

ACPD
10, 1193–1220, 2010

(SSA) (Dubovik and King, 2000). Accuracy of measurements is ∼0.01 for the AOD observations and ∼0.1 for SSA at AOD<0.2 (Dubovik et al., 2000). Further details about the AERONET products and relevant retrievals are available at the web site http://aeronet.gsfc.nasa.gov, where our measurements are accessible under the "Ev-K2-CNR" station page. A similar sunphotometer is installed by the AERONET at Gandhi College (GC, 26° N–84° E, 60 m a.s.l.) in the Gange's river plain, some 350 km SW to NCO-P (e.g., Fig. 1). Gandhi College observations are employed here as a proxy of aerosol conditions in the Indo-Gangetic basin, a region we will show as of likely origin of the anthropogenic aerosol reaching the Himalayas.

2.2 Backtrajectories

Ten-day NOAA-Hysplit backtrajectories (http://www.arl.noaa.gov/HYSPLIT.php) have been computed to identify the near-ground origin of the air-masses reaching the NCO-P during the observational period. In this analysis, Hysplit rather than Lagranto backtrajectories (as in Bonasoni et al., 2010) have been used to exploit codes successfully developed to detect Saharan dust origin by accounting for air-mass transits within the planetary boundary layer (PBL), e.g., Gobbi et al. (2004). In fact, PBL height is an output of the Hysplit model. Results of these runs include: 1) daily backtrajectory clusters ending at 300 and 600 m above the station at both 00:00 UTC (local 05:45 a.m.), and 12:00 UTC (local 05:45 p.m.), and 2) spatial density of all the back-trajectory transits within the PBL. We use this latter information to infer if transit of the air masses over a geographical region is potentially associated to an "entrainment" of local aerosols or pollutants, i.e., as a marker of the particulate matter origin. Backtrajectories are stopped when accumulating over 10 mm of rainfall (another Hysplit product) along their path. Since trajectories ending at 300 m and 600 m altitude resulted to be very similar, here we present the 600 m ones only. The origin density (percent of backtrajectories transiting within the PBL over 1×1-degree geographical pixels) of all the backtrajectories ending at 600 m a.g.l. at NCO-P in the period April 2006–March 2007 is summarized in Fig. 1. The same figure illustrates the location of both desert regions (shaded

areas) and fire events. The latters are given in terms of number, location and monthly distribution, as retrieved at a 1×1-degree resolution from the space-borne MODIS sensor (e.g., http://neo.sci.gsfc.nasa.gov/).

3 Results

As defined in Bonasoni et al. (2010), we address as "pre-monsoon" the period 1 March–20 May, as "monsoon" the period 21 May–26 September, and as "post-monsoon" the period 27 September–20 November 2006. The period 21 November 2006–31 January 2007 is then defined as "winter season".

3.1 Advection patterns

Ten-day Hysplit backtrajectories for the four above-defined periods are presented in Fig. 2. Both the backtrajectory patterns as a function of arrival day (colour coded), and the trajectory origin densities are plotted (left and right columns, respectively). Since the origin domains resulted to be much smaller than the full backtrajectory ones, a reduced geographical region is employed in the right column to represent all the source regions identified by our PBL-transit method. As anticipated by Fig. 1, this analysis shows that the most frequent PBL origin of airmasses reaching the NCO-P is situated in Nepal and at its borders with India and Bangladesh. Lagranto backtrajectories provided very similar results (Bonasoni et al., 2010). With the exception of the monsoon period, backtrajectories show that some long-range transport episodes are also possible. However, the trajectory origin plots (right column in Fig. 2) indicate that at these furthermost distances trajectories tend to travel in the free-troposphere, i.e., not entering the PBL. A few (frequency <10%) mid-range trajectories appear to originate in the Takla Makan desert (end of April 2006), Thar desert (1–20 April 2006), and Bangladesh-Gulf of Bengal, during the pre-monsoon period. Trajectories indicating the possible Thar and Takla Makan deserts origin in the pre-monsoon period well

ACPD
10, 1193–1220, 2010

agree with the dust advection patterns observed by Liu et al. (2008), and Gautam et al. (2009). However, the possibility that sub-grid transport processes not captured by back-trajectories could advect aerosols from far regions as the Arabic peninsula, and North Africa cannot be completely ruled out. An overview of dust transport episodes reaching NCO-P is given in a specific paper by Duchi et al. (2010).

With regard to biomass burning aerosols, Fig. 1 points out that fires (mostly due to agricultural practices) are set mainly in the period March–May and in October. In northern India, this practice is linked to the wheat-rice crop rotation performed in this area and generates large quantities of fine, BC rich aerosols (e.g., Badarinath et al., 2009). PBL backtrajectory origins for these two periods indicate that fire plumes are likely to be conveyed to NCO-P during the pre monsoon period from Northern India, Nepal and Bangladesh and, to a lesser extent, during the post monsoon from northern India. In the next section we shall verify the effectiveness of such transport patterns.

With the exception of a westerly transport in mid June, the monsoon season is characterized by short, rain-out-interrupted, back-trajectories mainly proceeding from SE and originating in the Eastern Nepal, East India and Bangladesh regions. A westerly, short-range circulation is re-established in the post monsoon. Trajectories then extend further to the west (up to North Africa and Europe) during the winter season. Still, the PBL-transit densities remain essentially confined to the Nepalese and northern India regions.

3.2 The sunphotometer observations

The statistics of the sunphotometer measurements at Ev-K2-CNR for the period April 2006–March 2007 are reported in Table 1. This shows that 24% of level 1.0 (L1), unscreened measurements were rejected by the cloud-screening process leading to the 7127 level 1.5 (L1.5) observations discussed here. Due to anabatic winds and consequent formation of afternoon clouds, the number of morning measurements at Ev-K2-CNR was on average 2.85 times the post-meridian one. Both the number of L1 daily measurements and percentage of L1.5 data during the five periods are illustrated

in Fig. 3. Because of significant cloud contamination, both the number of observations and inverted retrievals become rather low during the monsoon season. An instrumental failure caused the measurements gap visible in the period 11–24 February 2007.

Monthly medians of 500 nm AOD (also showing contribution of fine-mode particles, AOD_{FM}) and precipitable water (PW) data at both Ev-K2-CNR and GC are presented in Fig. 4 (top and bottom row, respectively). PW and AOD levels at Ev-K2-CNR are about one order of magnitude smaller than at GC, with typical wintertime AOD of the order of 0.05 and 0.75, respectively. To provide a comparison, the 3400 m a.s.l. background station of Mauna Loa (Hawai) recorded an average 500 nm AOD=0.011 and PW=0.17 cm in January 2007 and AOD=0.013 and PW=0.35 cm in August 2006. The PW records of Ev-K2-CNR and GC reveal the beginning and end of the wet, monsoon season (mid-May, end of September 2006, respectively) to proceed in phase at both stations. Conversely, AOD at NCO-P follows a seasonal cycle markedly different from the GC one, presenting a maximum in the summer (monsoon) season, mostly attributable to coarse-particle extinction. This does not occur at Gandhi College, where the AOD maximizes both in spring (mixture of fine (pollution) and coarse (mineral dust) particles, e.g., Chinnam et al., 2006; Prasad and Singh, 2007), and in winter (mostly fine mode pollution), while minimizing in summer (likely due to the monsoon rainout effect). Therefore, the coarse particle-driven summer maximum observed at NCO-P cannot be related to the advection of mineral dust from the IG plains. It is however interesting to notice similarities in the fine mode AOD time patterns of the two stations.

As pointed out in the discussion of Table 1, the number of afternoon measurements was smaller than the morning one because of clouds generated by anabatic winds (see also Bonasoni et al., 2010). Figure 5 summarizes the impact of such oscillation on various observed parameters. The a.m. vs. p.m. (with respect to local noon) behaviour of the median AOD, AOD_{FM} and AOD_{FM}/AOD at Ev-K2-CNR reported in Fig. 5 confirm an impact of the valley breeze regime on the air column above NCO-P. In fact, the p.m. AOD_{FM} (Fig. 5b) is larger than the a.m. one, in particular during the months of highest BC advection (Fig. 5d). The same is not always observed in the total AOD,

which will be shown to be affected by the presence of cirrus-like clouds. At ground level, the valley breeze regime is found to bring pollutants (such as BC and PM_1) to NCO-P all year round, with weaker intensity during the monsoon period (e.g., Marinoni et al., 2010). BC observations reported in Fig. 5d evidenced: a) maximum BC levels in the months of April and October 2006, plus in January, February and March 2007; and b) an afternoon to morning BC ratio always of the order of two or larger, with the exception of the monsoon period when, however, it remained larger than one. In this respect, we must remember that April and October are periods of maximum biomass residues burning in the IG region (e.g., Fig. 1). The backtrajectory patterns of Fig. 2 confirm these aerosols are likely advected to NCO-P during these periods.

In Fig. 6a we compare the 500 nm AOD daily-averaged time series to daily-averaged, 500 nm aerosol extinction coefficients (σ_{ext}), as computed from concurrent in-situ aerosol size-distributions data from the NCO-P optical particle counter (e.g., Marinoni et al., 2010). The σ_{ext} have been calculated by Mie theory, assuming a refractive index m=1.5–0.001i. This comparison provides information on the altitude dependence of the aerosol content. The plots show the two variables to be anti-correlated during the monsoon season, when the AOD reaches maximum yearly values and σ_{ext} minimum ones, both about an order of magnitude above/below the pre-monsoon levels. In Fig. 6a we also report the aerosol scale height H_a, a parameter used to characterize the commonly observed exponential decrease with height (z) of the aerosol extinction coefficient: $\sigma_{ext}(z)=\sigma_{ext}(0)\exp(-z/H_a)$. For such a vertical distribution, the integral over z of $\sigma_{ext}(z)$, i.e., the AOD, is linked to the ground extinction $\sigma_{ext}(0)$ by the simple relationship H_a=AOD/$\sigma_{ext}(0)$ (e.g., Tomasi, 1982; Kaufman and Fraser, 1983).

Typical tropospheric values of H_a lay in the range 0.3–3 km. Here at NCO-P we notice H_a to attain values smaller than 10 km only during the pre-monsoon season, to reach values of over 100 km during the monsoon, and start declining back to less than 10 km only past November 2006. In agreement with the previous AOD discussion, this behaviour suggests that elevated layers (cirrus cloud-like) strongly contribute at determining the (coarse particle-generated) AOD during the monsoon, post-monsoon

ACPD
10, 1193–1220, 2010

and winter seasons at NCO-P. In this respect, it is interesting to observe that the break in the monsoon occurred in the period 12–23 June 2006 (evidenced here by the blue backtrajectories in Fig. 2, and discussed in Bonasoni et al., 2008) led to an aerosol (σ_{ext}) increase at the ground and to a consequent decrease of H_a below 10 km.

The time evolution of the 440–870 nm Angstrom exponent (AE) at Ev-K2-CNR is plotted in Fig. 6b together with the 440 nm aerosol single scattering albedo (SSA is not retrieved by AERONET at 500 nm) observed at the two stations. Here we notice a rather stable behaviour of the SSA at GC (green diamonds), maintaining an average value of the order of 0.9±0.05 over the whole year. Conversely, SSA at Ev-K2-CNR (magenta stars) attains such values on a few days of the pre-monsoon season, while decreasing to unrealistically low values at the onset of the monsoon until the winter season. As guessed before, such a behaviour can be explained by the presence of "giant" (over 20 µm) particles the inversion algorithm is unable to reproduce, then attributing the relevant extinction to absorption processes (Oleg Dubovik, personal communication, 2009). The systematic presence of these large particles (likely cirrus or ice particles) suspended in the air column above NCO-P (particularly during the monsoon and post-monsoon seasons) appears then to be confirmed by this third element.

In early April and early May 2006, however, high Angstrom exponents (i.e., AE>1.5) do indicate the AOD (of the order of 0.03 at 500 nm) to be determined essentially by fine particles (i.e., no cirrus contamination). In these periods, the SSA of Fig. 6b present values in the range 0.6–0.9, i.e., in conformity with minimum SSA values observed at NCO-P by Marcq et al. (2010), and coinciding with the maximum in BC reported in Fig. 5d. These conditions indicate that in some days column SSA values as low as 0.6–0.7 (±0.1) might characterize aerosols at NCO-P. In fact, high aerosol absorption (SSA~0.78) was also observed by Ramana et al. (2004) during a winter campaign carried-out in Kathmandu and nearby locations.

According to the picture established so far, cirrus-like clouds appear to be more important than aerosols at determining the AOD and the consequent radiative forcing at NCO-P over a large part of the year. The rather low values both the Angstrom exponent and the AOD_{FM}/AOD ratio attain during most of the year can help defining the time progression of such condition. At the same time, pollution aerosols exhibit high absorption characteristics (SSA ranging from ∼0.9 down to ∼0.6. As indicated in the introduction, such SSA levels do lead to an atmospheric warming effect over most ground albedoes (Haywood and Boucher, 2000). In fact, the absolute value of this atmospheric forcing is expected to be moderated by the very low values of the AOD (e.g., Pant et al., 2006).

3.3 The altitude-resolved picture from satellite observations

To support the discussion of ground-based measurements presented so far we used observations from the CALIOP lidar onboard CALIPSO (the NASA-CNES Cloud-Aerosol Lidar and Infrared Pathfinder Satellite Observations) launched in April 2006 (Winker et al., 2007). These provide an opportunity to investigate the season-dependent vertical distribution of aerosols and thin clouds in this region. Since CALIOP observations started in June 2006, we miss such information for the pre-monsoon period. In Fig. 7 we show profiles from CALIPSO transects crossing within 200 km from NCO-P. The CALIOP lidar backscatter signals from the 532 nm cross and parallel-polarized channels are both plotted (left and right columns, respectively). Since spherical aerosols do not depolarize the laser beam they backscatter, the cross-polarized lidar signal is essentially originated by non-spherical particles as ice crystals and mineral dust (e.g., Gobbi et al., 2004). The image pairs of Fig. 7 then provide a picture of the shape-dependent aerosol load along each transect. Two principal features result from this CALIOP record: 1) the common piling-up of aerosols against the Himalayas, and 2) the recurrent presence of cirrus/ice clouds over the mountain range.

ACPD
10, 1193–1220, 2010

Figure 7a and b reports 13 and 25 June 2006 profiles, respectively. In spite of the ongoing monsoon season, the period of 12–23 June presented a shift in circulation (from SE to NW, e.g., Fig. 2) resulting into a break of the monsoon (Bonasoni et al., 2008). This brought clear skies and pollution build-up against the Himalayas, as shown in Fig. 7a, and confirmed by the extinction and scale height records in Fig. 6. Typical monsoon conditions, with extended cloud and/or cirrus cover over the whole transect where re-established on 25 June (Fig. 7b).

Formation of cirrus clouds above the Himalayas, following the uplift of polluted air-masses from the IG plain in the early post-monsoon season (6 October 2006), is depicted in Fig. 7c. In this case, presence of pollution and cirrus clouds is accompanied by an increase in ground extinction and a reduction in H_a at NCO-P (Fig. 6). However, the persistent small values of AOD_{FM} in the period October–December 2006 (e.g., Fig. 4), together with concurrent high aerosol scale heights, indicate that the cirrus-like cloud conditions as of Fig. 7c can also be common during the post-monsoon and winter seasons. Presence of cirrus clouds over the Himalayas is also shown by the 27 February 2007 (pre-monsoon) CALIOP transects of Fig. 7d.

As mentioned, one interesting outcome of the CALIOP profiles is the detection, in non-monsoon periods, of aerosols piling-up from the IG plains towards the Himalayan foothills (e.g., Figs. 7a, 5c, and d). This mechanism generates an impressive pollution "wave" the mountain range gets impacted by (along the trajectories illustrated in Fig. 2) and helps venting into the free troposphere. This also explains the very high concentration of black carbon (>1 μg/m^3) often observed at the NCO-P in the pre-monsoon season (e.g., Fig. 5, and Marinoni et al., 2010). During winter the depth of the pollution layer decreases as a consequence of reduced convection. However, Fig. 7 together with backtrajectories of Fig. 2 show that also in the cold season polluted air masses can travel from the IG plains to and over the remote, high altitude location of NCO-P.

ACPD
10, 1193–1220, 2010

4 Conclusions

The first year-round sunphotometer observations carried out at the high altitude (5079 m a.s.l.) Himalayan Nepal Climate Observatory – Pyramid showed both AOD and PW cycles to maximize during the monsoon season (May–September 2006, median 500 nm AOD∼0.14) and minimize (median AOD∼0.04) in winter. These AOD values are higher than the ones observed at the 3400 m a.s.l., background station of Mauna Loa (Hawaii) in the same periods: ∼0.013 and ∼0.011, respectively. The monsoon AOD maximum at Ev-K2-CNR is found to be caused mainly by large, supermicron particles. Conversely, in the Indo-Gangetic basin, some 300 km SW to NCO-P, the Gandhi College sunphotometer observed AOD to minimize during the monsoon, when most of the optical depth was generated by fine mode, submicron particles. In this respect, similarities are found between the fine mode AODs at the two stations, while the NCO-P coarse mode summer AOD maximum appears to be uncoupled from IG-plains emissions. This uncoupling was unexpected since backtrajectories indicate the NCO-P to be influenced by transport from the plains of Nepal and northern India during most of the year. With some exceptions in the pre-monsoon period, aerosol scale heights computed at NCO-P confirmed that it was elevated particle layers that regularly contributed at determining the local AOD, in particular its coarse fraction. This finding is also supported by the observations of the satellite lidar CALIOP, which reveals frequent presence of cirrus clouds over the Himalayas. The dual contribution to the AOD (from both low and elevated particle layers) complicates the assessment of the aerosols radiative impact in this region by hampering the retrieval of correct radiative parameters from sunphotometry. When retrievable, the SSA of fine mode aerosols resulted to be mostly below the threshold of 0.9, with minima of the order of 0.6, i. e., conditions certainly leading to a positive (warming) radiative forcing (Haywood and Boucher, 2000). However, the very low optical depths associated to periods characterized by absorbing aerosols (winter season and pre-monsoon) are expected to moderate such a warming (e.g., Pant et al., 2006).

The CALIOP lidar profiles also revealed pollution from the IG plains to accumulate against the Himalayas, up to altitudes of 4–5 km. With a minimum in the monsoon season, pollution (in the form of BC) was regularly observed to be advected by mountain breeze to NCO-P (Marinoni et al., 2010). In fact, backtrajectories indicate the Nepal and northern India plains regions to represent the most common origin of PBL-influenced airmasses reaching the NCO-P all year round. In April and October, backtrajectories were found to originate in areas of maximum agricultural fires, possibly explaining the very high levels of BC observed in these periods. Analysis of backtrajectory transits within the PBL also attributed long-range transport of mineral dust essentially to advection from the west Asian arid regions of the Thar and Takla Makan deserts and of Tibet. Even though pre-monsoon and winter season backtrajectories reached over the Arabian, North African and European regions, no trajectories were found to originate in the boundary layer of these areas.

Acknowledgements. This study was carried out within the framework of the Ev-K2-CNR "SHARE – Stations at High Altitude for Research on the Environment" Project, in collaboration with the Nepal Academy of Science and Technology. We thank the AERONET for supporting the NCO-P instrument, and for providing the Gandhi College data. We thank the NOAA-Air Resource Laboratory for making HYSPLIT accessible to the research community. We also thank the NASA Langley Research Center Atmospheric Science Data Center for open distribution of the CALIPSO/CALIOP data, and NASA Goddard Earth Sciences Data Center for distributing the MODIS data.

References

Badarinath, K. V. S., Kharol, S. K., and Sharma, A. R.: Long-range transport of aerosols from agriculture crop residue burning in Indo-Gangetic Plains: A study using LIDAR, ground measurements and satellite data, J. Atmos. Sol.-Terr. Phy., 71, 112–120, 2009.

Bellouin, N., Jones, A., Haywood, J., and Christopher, S. A.: Updated estimate of aerosol direct radiative forcing from satellite observations and comparison against the Hadley Centre climate model, J. Geophys. Res., 113, D10205, doi:10.1029/2007JD009385, 2008.

Bonasoni P., Laj, P., Cristofanelli, P., Sprenger, M., Decesari, S., Duchi, R., Angelini, F., Arduini, J., Bonafè, U., Calzolari, F., Colombo, T., Di Sarra, A., Evangelisti, F., Maione, M., Facchini, M. C., Fuzzi, S., Gobbi, G. P., Panday, A., Roccato, F., Sellegri, K., Venzac, H., Verza, G. P., Villani, P., Vuillermoz, E., and Marinoni, A.: Atmospheric Brown Clouds in the Himalayas: first two years of continuous observations at the Nepal-Climate Observatory at Pyramid (5079 m), Atmos. Chem. Phys. Discuss., in preparation, 2010.

Bonasoni, P., Laj, P., Angelini, F., Arduini, J., Bonafè, U., Calzolari, F. P., Cristofanelli, P., Decesari, S., Facchini, M. C., Fuzzi, S., Gobbi, G. P., Maione, M., Marinoni, A., Petzold, A., Roccato, F., Roger, J. C., Sellegri, K., Sprenger, M., Venzac, H., Verza, G. P., Villani, P., and Vuillermoz, E.: The ABC-Pyramid Atmospheric Research Observatory in Himalaya for aerosol, ozone and halocarbon measurements, Sci. Total Environ., 391, 252–261, 2008.

Chinnam, N., Dey, S., Tripathi, S. N., and Sharma, M.: Dust events in Kanpur, northern India: Chemical evidence for source and implications to radiative forcing, Geophys. Res. Lett., 33, L08803, doi:10.1029/2005GL025278, 2006.

Dey, S. and Tripathi, S. N.: Aerosol direct radiative effects over Kanpur in the Indo-Gangetic basin, northern India: Long-term (2001–2005) observations and implications to regional climate, J. Geophys. Res., 113, D04212, doi:10.1029/2007JD009029, 2008.

Dubovik, O. and King, M. D.: A flexible inversion algorithm for retrieval of aerosol optical properties from sun and sky radiance measurements. J. Geophys. Res., 105, 20673–20696, 2000.

Dubovik, O., Smirnov, A., Holben, B. N., King, M. D., Kaufman, Y. J., Eck, T. F., and Slutsker, I.: Accuracy assessments of aerosol optical properties retrieved from Aerosol Robotic Network (AERONET) Sun and sky radiance measurements, J. Geophys. Res., 105(D8), 9791–9806, 2000.

Dubovik, O., Holben, B., Eck, T. F., Smirnov, A., Kaufman, Y. J., King, M. D., Tanrè, D., and Slutsker, I.: Variability of absorption and optical properties of key aerosol types observed in worldwide locations, J. Atmos. Sci., 59, 590–608, 2002.

Duchi, R., Cristofanelli, P., Marinoni, A., Calzolari, F., Angelini, F., Vuillermoz, E., Verza, G. P., and Bonasoni, P.: Two years of mineral dust transport observations at the Nepal Climate Observatory – Pyramid, Atmos. Chem. Phys. Discuss., in preparation, 2010.

Forster, P., Ramaswamy, V., Artaxo, P., Berntsen, T., Betts, R., Fahey, D. W., Haywood, J., Lean, J., Lowe, D. C., Myhre, G., Nganga, J., Prinn, R., Raga, G., Schulz, M., and Van Dorland, R.: Changes in atmospheric constituents and in radiative forcing, in: Climate Change 2007: The Physical Science Basis. Contribution of Working Group I to the Fourth Assess-

ment Report of the Intergovernmental Panel on Climate Change, edited by: Solomon, S., Qin, D., Manning, M., Chen, Z., Marquis, M., Averyt, K. B., Tignor, M., and Miller, H. L., Cambridge University Press, Cambridge, UK and New York, NY, USA, 2007.

Gautam, R., Liu, Z., Singh, R. P., and Hsu, C.: Two contrasting dust-dominant periods over India observed from MODIS and CALIPSO data, Geophys. Res. Lett., 36, L06813, doi:10.1029/2008GL036967, 2009.

Gobbi, G. P., Barnaba, F., and Ammannato, L.: The vertical distribution of aerosols, Saharan dust and cirrus clouds in Rome (Italy) in the year 2001, Atmos. Chem. Phys., 4, 351–359, 2004, http://www.atmos-chem-phys.net/4/351/2004/.

Haywood, J. and Boucher, O.: Estimates of the direct and indirect radiative forcing due to tropospheric aerosols: a review, Rev. Geophys., 38, 513–543, 2000.

Holben, B. N., Eck, T. F., Slutsker, I., et al.: AERONET – A federated instrument network and data archive for aerosol characterization, Remote Sens. Environ., 66, 1–16, 1998.

Kaufman, Y. J. and Fraser, R. S.: Light extinction by aerosols during summer air pollution, J. Appl. Meteorol., 22, 1694–1706, 1983.

Liu, Z., Liu, D., Huang, J., Vaughan, M., Uno, I., Sugimoto, N., Kittaka, C., Trepte, C., Wang, Z., Hostetler, C., and Winker, D.: Airborne dust distributions over the Tibetan Plateau and surrounding areas derived from the first year of CALIPSO lidar observations, Atmos. Chem. Phys., 8, 5045–5060, 2008, http://www.atmos-chem-phys.net/8/5045/2008/.

Marinoni, A., Cristofanelli, P., Duchi, R., Calzolari, F., Decesari, S., Sellegri, K., Laj, P., Vuillermoz, E., Verza, G. P., and Bonasoni, P.: Aerosol mass and black carbon concentrations at NCO-P, Atmos. Chem. Phys. Discuss., in preparation, 2010.

Nakajima, T., Yoon, S.-C., Ramanathan, V., et al.: Overview of the atmospheric brown cloud east asian regional experiment 2005 and a study of the aerosol direct radiative forcing in east Asia, J. Geophys. Res., 112, D24S91, doi:10.1029/2007JD009009, 2007.

O'Neill, N. T., Eck, T. F., Smirnov, A., Holben, B. N., and Thulasiraman, S.: Spectral discrimination of coarse and fine mode optical depth, J. Geophys. Res., 108(D17), 4559, doi:10.1029/2002JD002975, 2003.

Pant, P., Hegde, P., Dumka, U. C., Sagar, R., Satheesh, S. K., Moorthy, K. K., Saha, A., and Srivastava, M. K.: Aerosol characteristics at a high-altitude location in central Himalayas: Optical properties and radiative forcing, J. Geophys. Res., 111, D17206, doi:10.1029/2005JD006768, 2006.

Prasad, A. K. and Singh, R. P.: Changes in aerosol parameters during major dust storm events (2001–2005) over the Indo-Gangetic Plains using AERONET and MODIS data, J. Geophys. Res., 112, D09208, doi:10.1029/2006JD007778, 2007.

Ramana, M. V., Ramanathan, V., Podgorny, I. A., Pradhan, B. B., and Shrestha, B.: The direct observations of large aerosol radiative forcing in the Himalayan region, Geophys. Res. Lett., 31, L05111, doi:10.1029/2003GL018824, 2004.

Ramanathan, V. and Crutzen, P.: New directions: atmospheric brown "clouds", Atmos. Environ., 37, 4033–4035, 2003.

Ramanathan, V., Ramana, M. V., Roberts, G., Kim, D., Corrigan, C., Chung, C., and Winker, D.: Warming trends in Asia amplified by brown cloud solar absorption, Nature, 448, doi:10.1038/nature06019, 2007.

Ramanathan, V., Li, F., Ramana, M. V., Praveen, P. S., Kim, D., Corrigan, C. E., Nguyen, H., Stone, E. A., Schauer, J. J., Carmichael, G. R., Adhikary, B., and Yoon, S. C.: Atmospheric brown clouds: Hemispherical and regional variations in long range transport, absorption and radiative forcing, J. Geophys. Res., 112, D22S21, doi:10.1029/2006JD008124, 2007.

Ramanathan, V. and Carmichael, G. R.: Global and regional climate changes due to black carbon, Nature Geosci., 1, 221–227, doi:10.1038/ngeo156, 2008.

Satheesh, S. K. and Ramanathan, V.: Large differences in tropical aerosol forcing at the top of the atmosphere and Earth's surface, Nature, 405, 60–63, 2000.

Shrestha, A. B., Wake, C. P., Dibb, J. E., Mayewski, P. A., Whitlow, S. I., Carmichael, G. R., and Ferm, M.: Seasonal variations in aerosol concentrations and compositions in the Nepal Himalaya, Atmos. Environ., 34, 3349–3363, 2000.

Tomasi, C.: Features of the scale height for particulate extinction in hazy atmospheres, J. Appl. Meteorol., 21, 931–944, 1982.

Verma, S., Venkataraman, C., and Boucher, O.: Origin of surface and columnar Indian Ocean Experiment (INDOEX) aerosols using source- and region-tagged emissions transport in a general circulation model, J. Geophys. Res., 113, D24211, doi:10.1029/2007JD009538, 2008.

Wake, C. P., Mayewski, P. A., Zichu, X., Ping, W., and Zhongqin, L.: Regional distribution of monsoon and desert dust signals recorded in Asian glaciers, Geophys. Res. Lett., 20(14), 1411–1414, 1993.

Winker, D., Hunt, W., and McGill, M.: Initial performance assessment of CALIOP, Geophys. Res. Lett., 34, L19803, doi:10.1029/2007GL030135, 2007.

Table 1. Number of direct-sun measurements performed at Ev-K2-CNR in the period April 2006–March 2007. L1 and L1.5 indicate unscreened and cloud-screened observations, respectively.

	L 1	L 1.5	L1.5/L1
Total measures	9345	7127	0.76
Morning (a.m.)	6699	5276	0.79
Afternoon (p.m.)	2646	1851	0.70
Ratio a.m./p.m.	2.28	2.85	

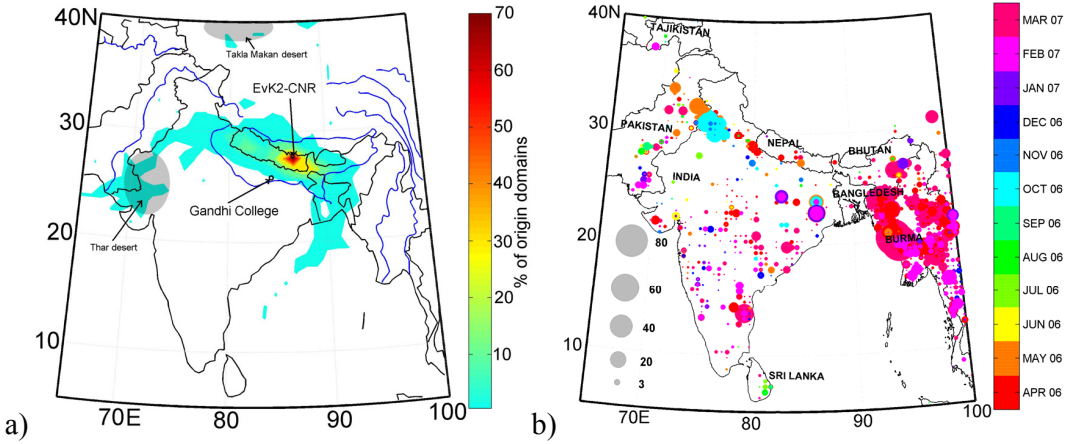

Fig. 1. **(a)** Location of the Ev-K2-CNR (at NCO-P) and Gandhi College (GC) AERONET stations and (colour-coded) PBL transit density of all the backtrajectories ending 600 m a.g.l. at NCO-P in the period April 2006–March 2007 (see Sect. 2.2 for details on backtrajectories); **(b)** monthly averages of fire counts per 1000 km^2 per day as observed by MODIS Terra. Bullet size identifies the number of fires, colour code the relevant month.

ACPD
10, 1193–1220, 2010

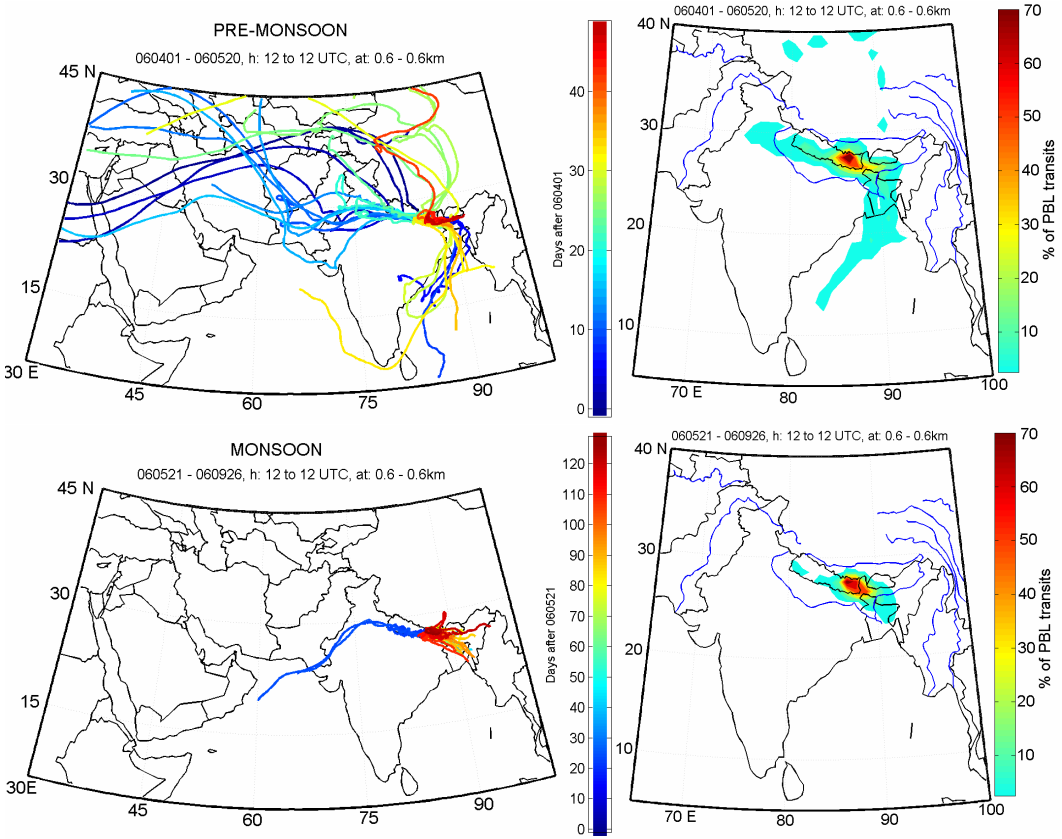

Fig. 2. Left column: daily patterns (colour-coded time scale) of back-trajectories ending at 12:00 UTC, 600 m above NCO-P during the 2006–2007 pre-monsoon, monsoon, post-monsoon, and winter season periods (first to fourth row, respectively). Right column: corresponding contour plots of the back-trajectories origin density (evaluated as percent of trajectory transits in the local PBL).

ACPD
10, 1193–1220, 2010

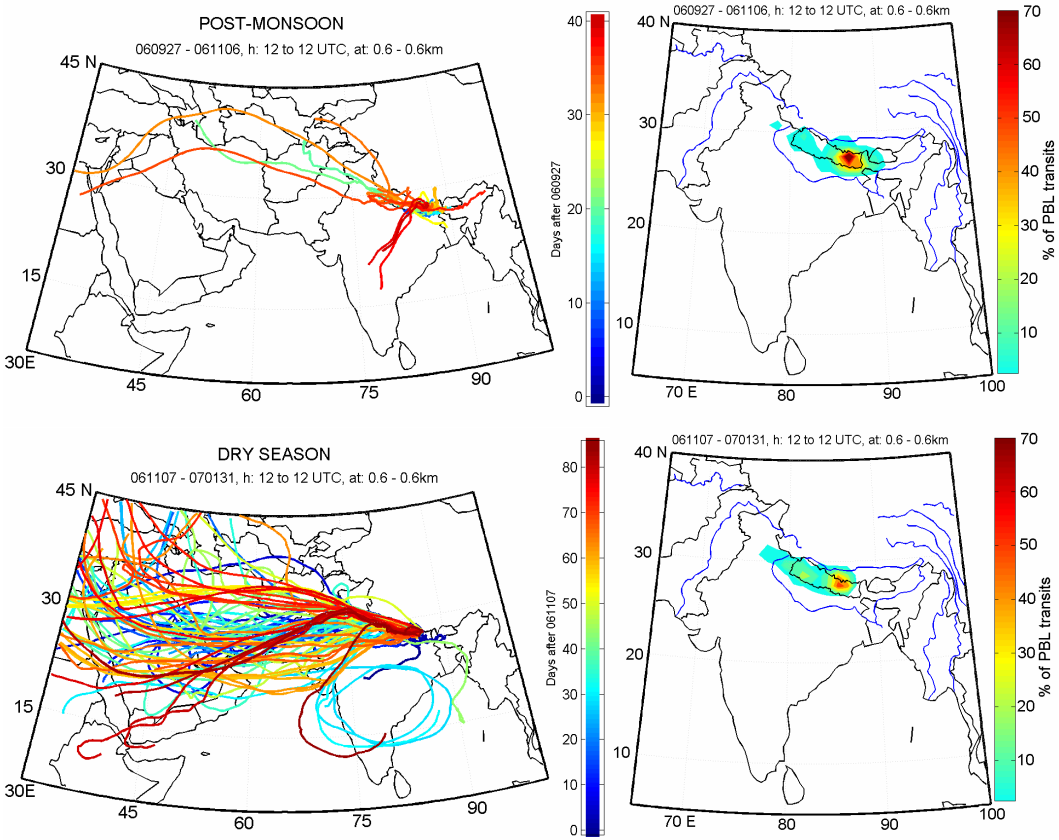

Fig. 2. Continued.

ACPD
10, 1193–1220, 2010

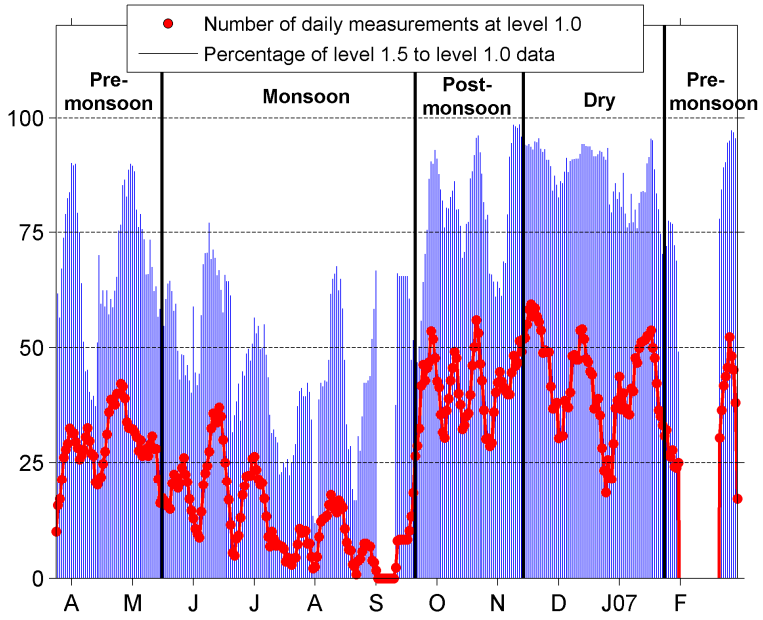

Fig. 3. Number of L1 sunphotometer measurements per day at the Ev-K2-CNR (red dots) and percent of cloud-screened, L1.5 data (blue bars) in the period April 2006–March 2007.

ACPD
10, 1193–1220, 2010

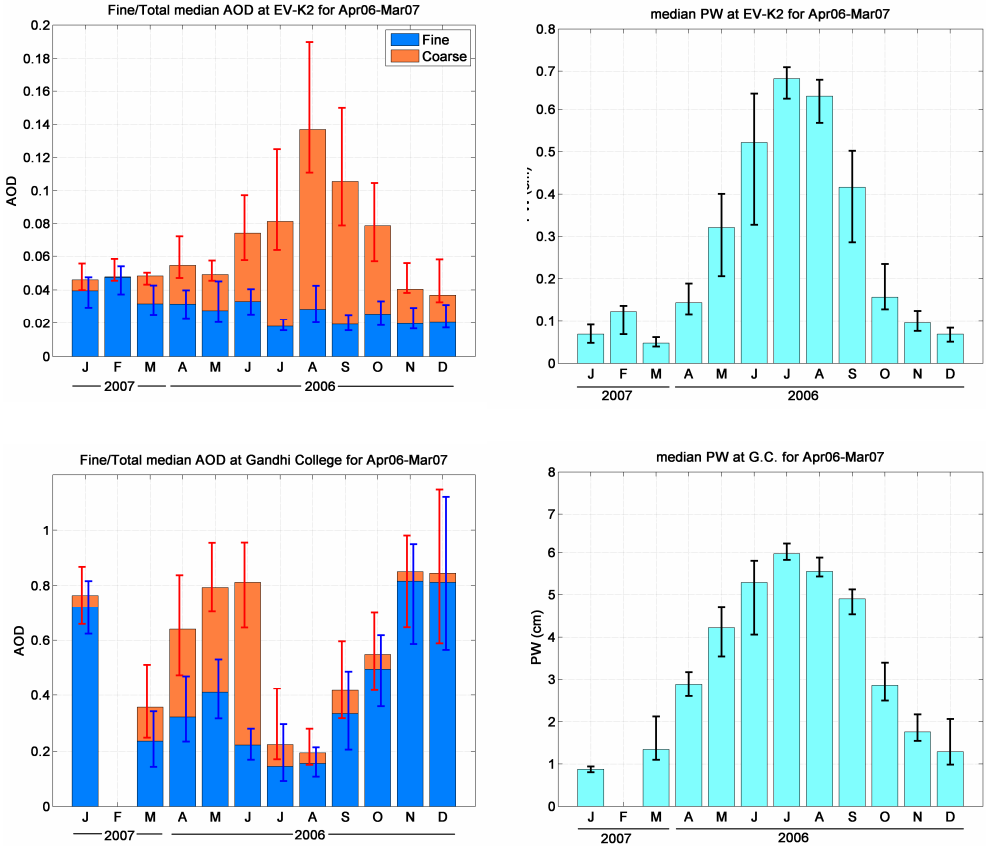

Fig. 4. Monthly median sunphotometer observations collected in the period April 2006–March 2007 at Ev-K2-CNR (top row) and Gandhi College (bottom row). L1.5, cloud-screened 500 nm AOD (blue bars) and contribution of fine-mode particles, AOD_{FM} (orange bars) are plotted in the left column, while precipitable water (PW) plots are in the right column. Thin lines span the 25th–75th percentile intervals.

ACPD
10, 1193–1220, 2010

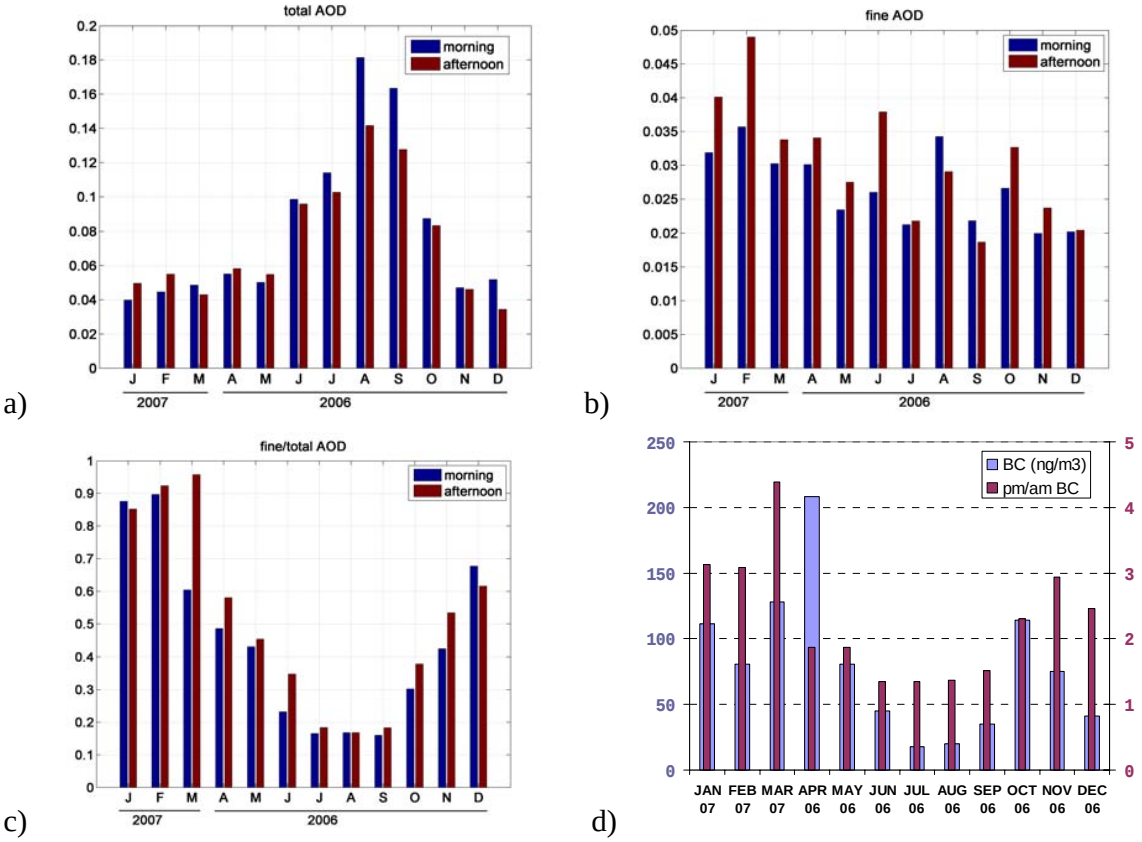

Fig. 5. Ev-K2-CNR monthly medians of morning (blue bars) and afternoon (red bars) sunphotometer observations of: **(a)** total AOD, **(b)** fine mode AOD, **(c)** fine to total AOD ratio. In **(d)** purple bars report the median black carbon content (ng/m^3, left axis) and the afternoon/morning black carbon ratio (red bars, right axis) measured at ground level at NCO-P.

ACPD
10, 1193–1220, 2010

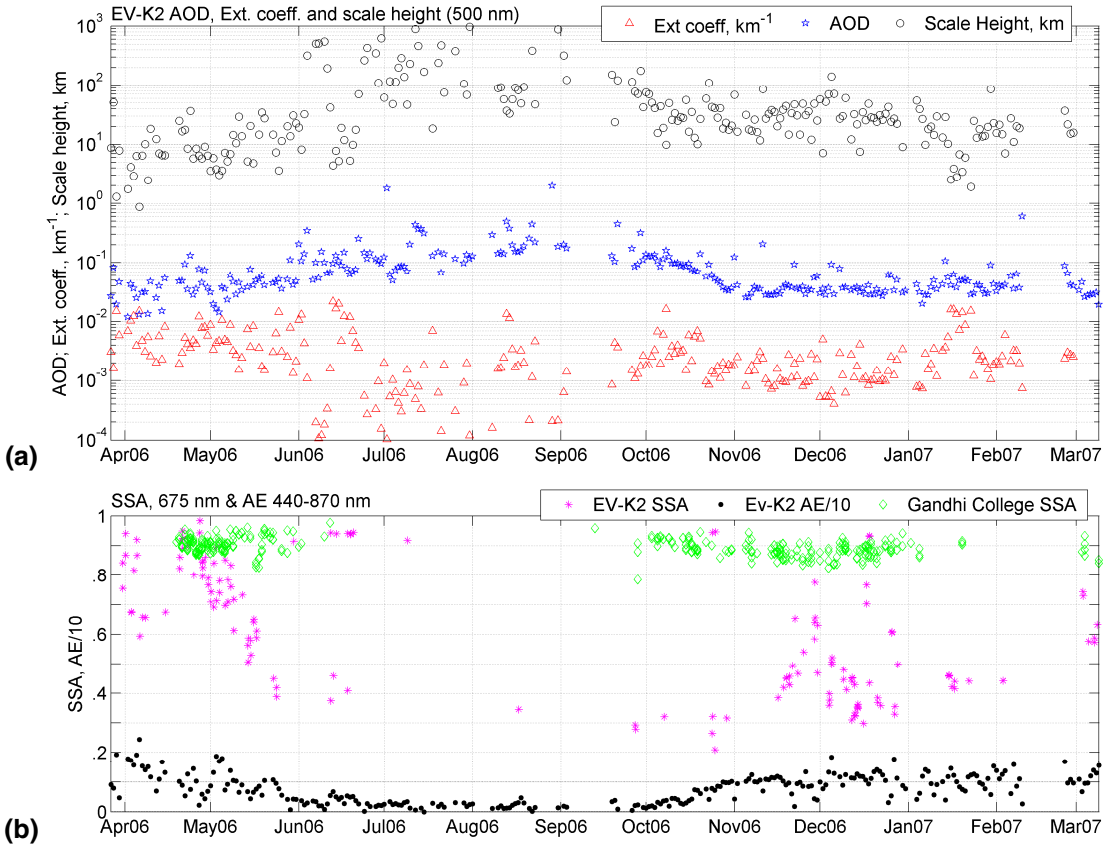

Fig. 6. **(a)** Daily-average values of: 500 nm AOD (blue stars); 500 nm ground aerosols extinction coefficient (red triangles), and aerosol scale height H_a (black circles) observed at the NCO-P; **(b)** daily-average values of: the 440–870 nm Angstrom exponent (AE, divided by 10) at Ev-K2-CNR (black dots) and 440 nm aerosol single scattering albedo at Ev-K2-CNR (magenta stars), and at Gandhi College (green diamonds).

ACPD
10, 1193–1220, 2010

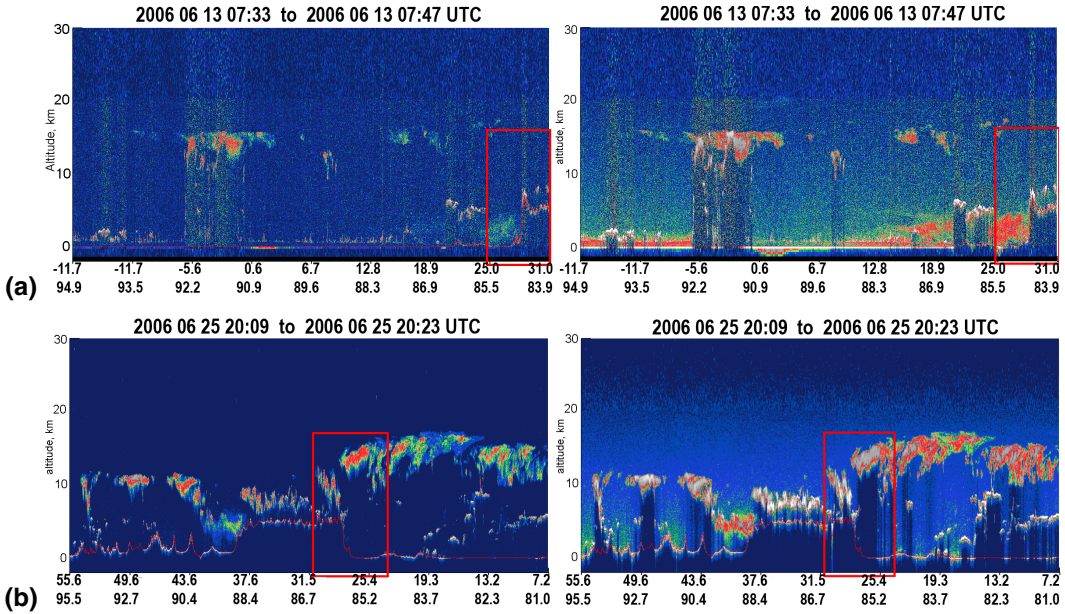

Fig. 7. CALIOP lidar transects across the Himalayas on 13 June 2006 **(a)**, 25 June 2006 **(b)**, 6 October 2006 **(c)**, and 27 February 2007 **(d)**. The first lines of abscissa labels indicate the latitude, the second the longitude. Cross and parallel-polarized lidar returns (in terms of attenuated backscatter coefficients) are presented in the left and right columns, respectively. The Himalayan region is evidenced by a red box.

ACPD
10, 1193–1220, 2010

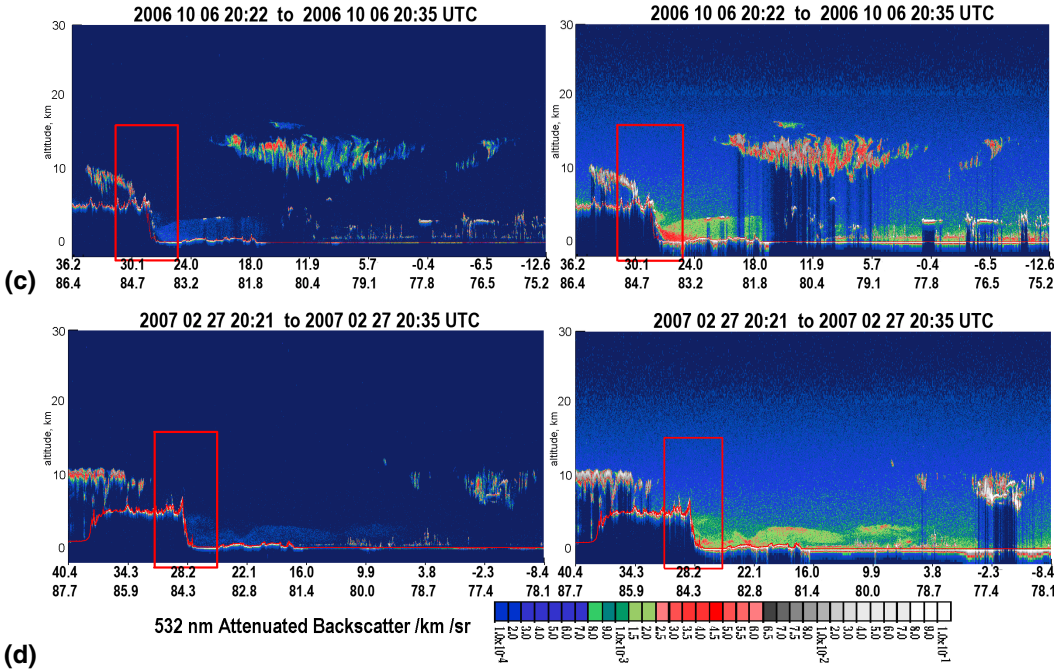

Fig. 7. Continued.

ACPD
10, 1193–1220, 2010